Journal of Neuroscience Methods 350 (2021) 109043

Contents lists available at ScienceDirect

Journal of Neuroscience Methods

journal homepage: www.elsevier.com/locate/jneumeth

Novel method to produce a layered 3D scaffold for human pluripotent stem cell-derived neuronal cells

Laura Honkamäki [a,*], Tiina Joki [a], Nikita A. Grigoryev [b], Kalle Levon [b], Laura Ylä-Outinen [a,1], Susanna Narkilahti [a,1]

[a] NeuroGroup, Faculty of Medicine and Health Technology, Tampere University, Tampere, Finland
[b] Department of Chemical and Biomolecular Engineering, NYU Tandon School of Engineering, Brooklyn, NY, USA

ARTICLE INFO

Keywords:
Collagen 1
Electrospinning
Guidance cue
Hydrogel
Polylactide
Tissue engineering

ABSTRACT

Background: Three-dimensional (3D) in vitro models have been developed into more in vivo resembling structures. In particular, there is a need for human-based models for neuronal tissue engineering (TE). To produce such a model with organized microenvironment for cells in central nervous system (CNS), a 3D layered scaffold composed of hydrogel and cell guiding fibers has been proposed.
New method: Here, we describe a novel method for producing a layered 3D scaffold consisting of electrospun poly (L,D-lactide) fibers embedded into collagen 1 hydrogel to achieve better resemblance of cells' natural microenvironment for human pluripotent stem cell (hPSC)-derived neurons. The scaffold was constructed via a single layer-by-layer process using an electrospinning technique with a unique collector design.
Results: The method enabled the production of layered 3D cell-containing scaffold in a single process. HPSC-derived neurons were found in all layers of the scaffold and exhibited a typical neuronal phenotype. The guiding fiber layers supported the directed cell growth and extension of the neurites inside the scaffold without additional functionalization.
Comparison with existing methods: Previous methods have required several process steps to construct 3D layer-by-layer scaffolds.
Conclusions: We introduced a method to produce layered 3D scaffolds to mimic the cell guiding cues in CNS by alternating the soft hydrogel matrix and fibrous guidance cues. The produced scaffold successfully enabled the long-term culture of hPSC-derived neuronal cells. This layered 3D scaffold is a useful model for in vitro and in vivo neuronal TE applications.

1. Introduction

Tissue engineering (TE) and in vitro models have provided new insights into tissue functions and the development of novel treatments for diseases and trauma. TE aims for applications which resemble tissue in vivo as precisely as possible in certain perspective by combining biology, cell technology, biomaterial sciences, and engineering. In the TE applications it is important to include the components of the cells' natural microenvironment: extracellular matrix (ECM), surrounding cells and biochemical molecules for example growth factors. This enables mimicking cells' interaction with their microenvironment and their response to the physical and biochemical cues it offers (Hopkins et al., 2015; Huang et al., 2017). In vivo, cells have also organized, tissue specific microenvironment which provides them cues, guidance cues among others, for different cellular functions. Guidance cues in vivo can be mechanical contact guidance of ECM components, other cells or tissue structures (e.g. vascular structures) or guidance via concentration gradient of soluble factors (Berzat and Hall, 2010; Chen, 2019). Especially in the central nervous system (CNS), consisting of the brain and spinal cord, the cell's microenvironment is complex and highly organized and thus difficult to mimic in vitro. In the adult brain guidance cues are present as interconnectivity of different brain regions via aligned neural tracks such as white matter tracks (Tang-Schomer et al., 2014; Wedeen et al., 2012), and in the spinal cord as directed growth of axons (Hopkins et al., 2015). In addition, during the development of CNS, ECM components play significant role in guiding neural cell

* Corresponding author.
E-mail address: laura.honkamaki@tuni.fi (L. Honkamäki).
[1] These authors contributed equally.

https://doi.org/10.1016/j.jneumeth.2020.109043
Received 10 July 2020; Received in revised form 10 December 2020; Accepted 11 December 2020
Available online 17 December 2020

migration, differentiation and axonal growth (Bandtlow and Zimmermann, 2000).

Currently, 3D in vitro models are of high interest in disease modelling and drug screening (Benam et al., 2015). They can fill the gap between conventional 2D cell cultures and in vivo models, and they can offer insights into human-specific functions without translation from animal to human physiology (Hopkins et al., 2015). To study human cell interactions with other cells or with their surroundings in the CNS, human-based tissue or cellular material is needed; however, natural human neural tissue is difficult to obtain (Choi et al., 2017). To mimic tissue-like microenvironment of the neuronal cells, the proper components must be included to the model. As the CNS tissue is extremely soft, hydrogels offer potential material for in vitro neuronal models (Karvinen et al., 2018; Koivisto et al., 2017; Ylä-Outinen et al., 2019). Nevertheless, they typically lack guiding cues that are present in the tissue microenvironment and therefore for example composite materials including fibrous component are used or biochemical molecules for chemotaxis are added (Hopkins et al., 2015). However, it has to be bear in mind that current 3D in vitro models are still simplified, cell-based models for studying some certain cellular functions not all the functions occurring in neural tissue in vivo (Hopkins et al., 2015). Thus, there is a need to develop more reliable human cell-based 3D in vitro tools in that sense.

It has been shown that neurons respond to environments which topography resembles their natural microenvironment, even without the presence of additional biological cues (Johnson et al., 2018; Karvinen et al., 2018; Richardson et al., 2011; Ylä-Outinen et al., 2010). Several studies have used electrospun fibers on the micro- or nanometer scale to mimic the fibrous properties of the cellular microenvironment in neuronal in vitro applications. (Cao et al., 2009; Hyysalo et al., 2017; Schaub et al., 2016; Wang et al., 2010). At present, the 3D bioprinting is a rising technique in the field of TE due to its superior possibilities to form hierarchical structures. However, its current resolution is in a range of 50−400 μm (Qiu et al., 2020) and therefore does not yet correspond to the scale of cells, their processes or ECM components. Electrospinning is a versatile and simple technique that is used to produce fibrous scaffolds with a high surface area to volume ratio, controllable pore size and different fiber orientations and hierarchical structures (Papadimitriou et al., 2020). By varying the collector type, fibers of different orientations, e.g., random mesh or highly parallel aligned fibers, have been produced (Park et al., 2007). Both random and parallel aligned fibers have been used as topographical surfaces for neurite outgrowth and for neural differentiation of human pluripotent stem cells (hPSCs) (Cembran et al., 2020; Hyysalo et al., 2017; Johnson et al., 2018; KarbalaeiMahdi et al., 2017; Wieringa et al., 2019; Ylä-Outinen et al., 2010). The parallel aligned electrospun fibers can elongate and direct neurite outgrowth in 3D as they offer contact guidance for the neurons (Schaub et al., 2016). The electrospun fibers can be used as 3D scaffolds; however, the packing density of the fiber mesh may be too high for cells to spread throughout the scaffold (Bosworth et al., 2013; Jun et al., 2018), which can be overcome by embedding the fibers into a low-density hydrogel (McMurtrey, 2014).

Hence, it has been hypothesized that composite scaffolds of hydrogel and electrospun fibers combine both advantages: the softness of the hydrogel and the structural support and guidance cues of the fibrous scaffold. Several different 3D cell culture models integrating electrospun fibers with hydrogels have been reported (Bosworth et al., 2013). These models have been constructed, for instance, by restraining parallel aligned fiber layers between two polydimethylsiloxane rings and forming chambers for hydrogel-containing neuroblastoma cells (McMurtrey, 2014). The cells were spatially distributed throughout the structure; however, only one fiber layer was included in this scaffold (McMurtrey, 2014). The simplest method to realize multilayered scaffolds has been achieved by stacking portable random or parallel aligned fiber sheets and hydrogels with a layer-by-layer method. This type of scaffold has been shown to result in controlled orientation of rodent-derived glial cells (Weightman et al., 2014a), human corneal fibroblasts, and bovine nucleus pulposus cells (Yang et al., 2011). In these studies, fibers were attached to separate, square-shaped acetate frames, and cells were pre-seeded on the layers before gelation of the hydrogel, restricting cell growth to the fiber layer in the resulting multilayered scaffold. Thus, previous methods used separately electrospun fiber meshes and construction of the 3D scaffold afterwards. In addition, human-derived neuronal cells have not been used with layered scaffolds, although their use is essential for establishing reliable in vitro human models.

In this study, we describe a novel method for constructing a layered 3D scaffold to achieve an improved artificial microenvironment for hPSC-derived neurons. We are mimicking especially the effect of the microenvironment to cells behavior. The neurons responses to the surrounding factors, e.g. guidance cues are evaluated and referred here as tissue mimicry. The novelty of the method is based on the development of a rotating dual electrode collector and collecting the fibers to the substrate, which is positioned horizontally between the electrodes. The system enabled electrospinning of highly aligned poly(L,D-lactide) (PLA) fibers directly on top of freshly prepared collagen type 1 hydrogel embedded with hPSC neurons in a layered manner. With this design, the embedded cells did not directly face the voltage between the needle and collector (Grigoryev and Levon, 2018). Here, we constructed a 3D scaffold consisting of three parallel aligned fiber layers within a 3D hydrogel matrix. The scaffolds with HPSC-derived neurons were cultured for two weeks. The effect of the fibers on the guided growth of neurons was evaluated by analyzing the orientation of the single neurons near the fiber layer. The results showed that the fiber layers increased the directed cell growth and the extension of the neurites without additional functionalization. Hence, we successfully developed a layered 3D scaffold consisting of electrospun fiber layers embedded in hydrogel for neuronal in vitro applications.

2. Materials and methods

2.1. Electrospinning PLA fibers

The electrospinning method was based on a previously published method (Grigoryev and Levon, 2018), which was optimized here by switching the collector system from a vertical to horizontal plane. Additionally, the unique collector is an in-house developed, rotating collector with two parallel electrodes (Grigoryev and Levon, 2018), patent US10589451B2). It enables the production of highly aligned, thin fibers and transfers them to the substrate, deposited to the void between the electrodes. The polymer, PLA 96/4 molar ratio copolymer (Purasorb PLD 9620, Corbion Purac, Netherlands) at a concentration of 9.0 % (m/v) was dissolved into a 7:3 mixture of dichloromethane (Merck Millipore, USA) and dimethylformamide (Sigma Aldrich, USA) by stirring overnight at room temperature (RT). To produce PLA fibers with fluorescent labels, 0.1 % (v/v) FluoSphere fluorescent nanoparticles (ø = 0.2 μm, excitation/emission wavelength far red 660/680, Invitrogen, USA) were added to the polymer solution prior to electrospinning. Parallel aligned fibers were produced by the electrospinning process using a commercial SKE E-Fiber Electrospinning device (Leonardinos, Italy). The polymer solution was injected through a 22 Ga sharp tip needle with a flow rate of 0.4 ml/h using a syringe pump. A voltage of 15 kV was applied with a high voltage DC power supply with the needle acting as the positive electrode. Fibers were collected with custom-made, grounded, fork-shaped, rotating dual electrode collector made of stainless steel. The distance between parallel electrodes was 50 mm. The dual electrode collector was rotated at 1548 rpm (maximum speed of the system used). The collector mechanically transferred fibers to the sample holder, which consisted of a grounded metal plate and microscope slide with two 22 × 22 mm cover slips. The distance between the needle and the collector was 120 mm. Parameters were adjusted to obtain highly aligned, uniform fibers. The whole electrospinning system was encased in a fume hood to protect the user from the

evaporating solvent. The system setup is shown in Supplementary Fig. 1 and Supplementary video 1.

2.2. Scanning electron microscope

PLA fibers were characterized with field-emission scanning electron microscopy (FE-SEM). First, the fibers were coated with carbon sputtering and imaged with Zeiss UltraPlus FE-SEM in high vacuum at 3 kV. For characterization, four samples were imaged, and 100 fibers were measured (ImageJ software).

2.3. Preparation of collagen hydrogel

Collagen type 1 (Col1, rat tail, Gibco, ThermoFisher Scientific, USA) solution was used as a hydrogel scaffold in this study. Col1 hydrogel was prepared using the manufacturer's protocol. In brief, the Col1 stock solution (3 mg/mL) was neutralized with 1 M sodium hydroxide, diluted with 1 × phosphate buffered saline (PBS) to a final concentration of 0.5 mg/ml and kept on ice prior to gelation. Gelation of Col1 solution is temperature-responsive and occurs at 37 °C after neutralization of an acidic stock solution. The same Col1 solution was used for coating 2D control PLA fibers, for which a thin coating procedure was adapted from the manufacturer. In brief, Col1 stock solution (3 mg/mL) was diluted with 20 mM acetic acid to achieve a final Col1 concentration of 5 μg/cm^2. The solution was incubated on the fibers for one hour at RT. Then, the solution was removed, and the samples were washed three times with cell culture medium and used immediately.

2.4. Assembly of layered 3D scaffold and control scaffolds

The layered 3D scaffold with multiple fiber and hydrogel layers was constructed in a layer-by-layer manner using a unique, rotating, dual electrode collector. First, parallel aligned PLA fibers were electrospun on the sample holder as described above. The even and uniform fiber density was achieved with 5 min of electrospinning. The fibers were pre-wetted for five minutes with cell culture medium which was pipetted as a drop on the fibers and spread with self-made spherical stamp. Then, 50 μl of Col1 hydrogel solution was cast on the pre-wetted fibers and gelation occurred in a heated, humified chamber at 37 °C within 20 min. A new layer of fibers was electrospun on top of hydrogel, which was followed by another layer of hydrogel with similar gelation, and a final layer of fibers. The complete structure contained three fiber layers and two Col1 hydrogel layers (see Supplementary Fig. 2). Overall, the preparation of the layered 3D scaffold took approximately two hours including electrospinning and hydrogel gelation steps. The fiber layers were each thin and sparse and were practically embedded into the hydrogel. Therefore, hydrogel, as well as cells, surrounded the fibers. A schematic image of the structure is presented in Fig. 1A. To clarify the terminology, the fiber layer indicates an aligned oriented fiber layer in the hydrogel (thickness average 15.0 μm ± 5.0 μm) and a hydrogel layer without fibers in between fiber layers (Fig. 1A). In this study, two control groups were used. First, Col1-coated electrospun fibers were used as a 2D control (2D fiber, Fig. 1B). Moreover, the Col1 hydrogel scaffold without fibers acted as a 3D control (3D hydrogel, Fig. 1C).

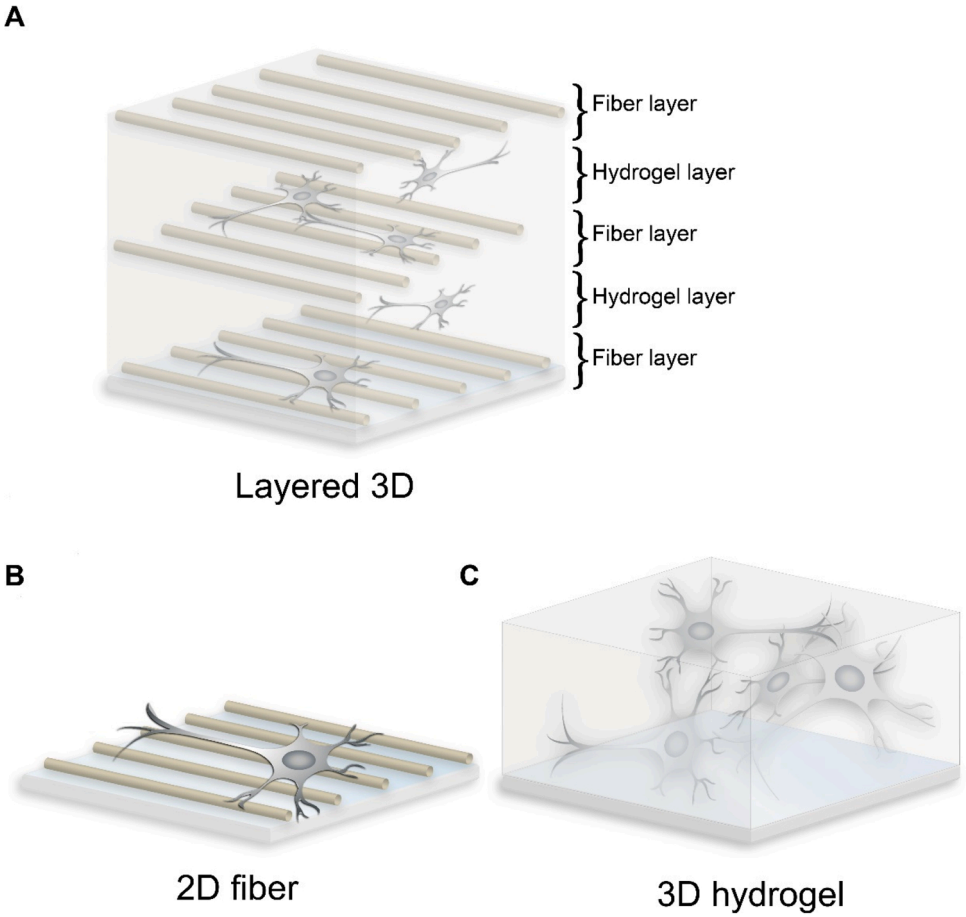

Fig. 1. Layered 3D scaffold and experimental groups. Schematic image of A) layered 3D scaffold (layered 3D) and neuronal cells growing inside the scaffold, B) 2D control fibers (2D fiber) and neuronal cells growing on top of the fibers, and C) 3D control hydrogel (3D hydrogel) and neuronal cells growing inside the hydrogel.

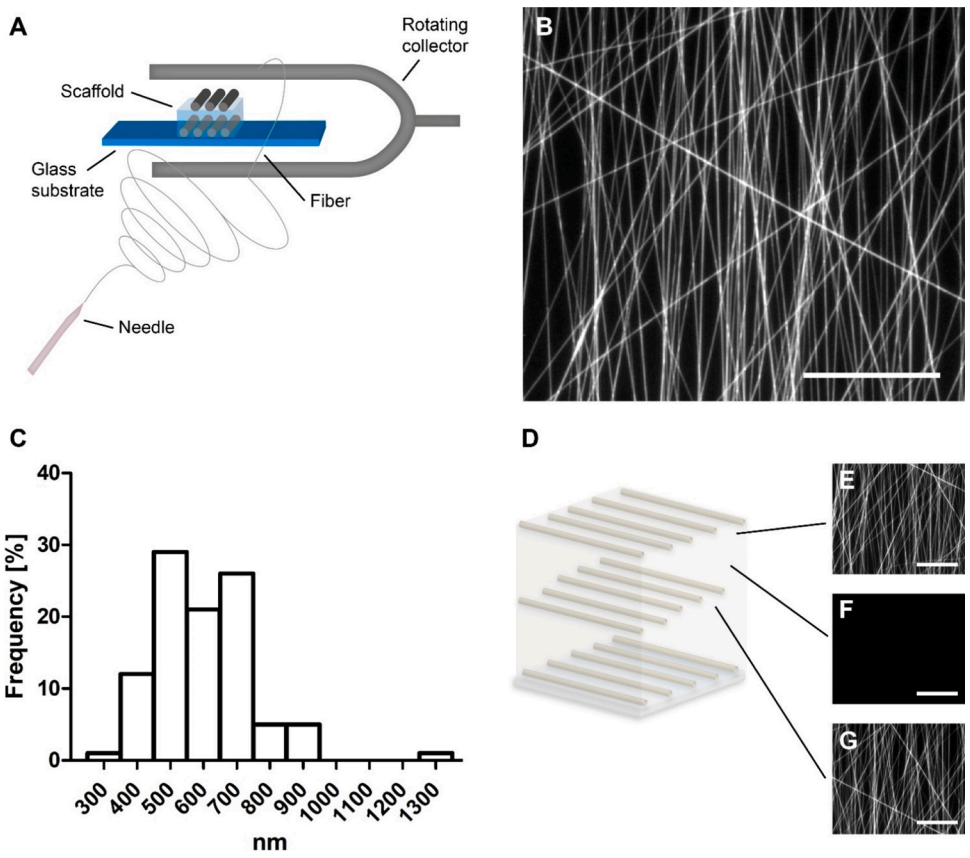

Fig. 2. Preparation of the layered 3D scaffold. A) Schematic image of the electrospinning setup and layer-by-layer preparation of the sample. In practice, there were two samples per microscopy slide processed at the same time. B) Fluorescence image showing fluorescent labeling of the electrospun fibers. The scale bar is 100 μm. C) Histogram showing fiber diameter distribution, n = 100. D) Schematic image depicting different layers of the layered 3D scaffold. E-G) Fluorescence microscopy images illustrate the separate fibers containing layers (E and G, average thickness 15.0 μm ± 5.0 μm) and the empty hydrogel layer between them (F). The scale bar is 100 μm.

2.5. Cells and differentiation

Human induced pluripotent stem cell (hiPSC) line (10212.EURCCs, derived in-house, Kiamehr et al., 2019) was used to produce neuronal cells. The HiPSC line was cultured in feeder-free conditions prior to differentiation into neurons using a previously published protocol (Hyvärinen et al., 2019). Neuronal differentiation was performed in laminin-coated wells (15 μg/μL, Laminin LN521, BioLamina, Sweden). Neural precursor cells were cultured in neural maintenance medium composed of 1:1 DMEM/F12 with Glutamax and Neurobasal, 0.5 % N2, 1.0 % B27 with retinoic acid, 0.5 mM GlutaMAX, 0.5 % NEEA, 50 μM 2-mercaptoethanol, 0.1 % penicillin/streptomycin (all purchased from Thermo Fisher Scientific) and 2.5 μg/ml insulin (Sigma Aldrich). Neural differentiation was induced (days 1–12) with 100 nM LDN193189 and 10 μM SB431542 (both purchased from Sigma Aldrich). For the neural proliferation stage (days 13–25), the medium was supplemented with 20 ng/ml fibroblast growth factor-2 (FGF2, ThermoFischer Scientific), and for the neural maturation stage (days 26–130), the neural maturation medium (NMM) was supplemented with 20 ng/ml brain-derived neurotrophic factor (BDNF, R&D Systems, USA), 10 ng/ml glial-derived neurotrophic factor (GDNF, R&D Systems), 500 μM dibuturyl-cyclicAMP (db-cAMP, Sigma-Aldrich) and 200 μM ascorbic acid (AA, Sigma-Aldrich). At day 32, cells were plated for experiments. Most of the cells produced with this protocol are neurons with a minor portion of astrocytes (Hyvärinen et al., 2019). All cultures were maintained at 37 °C in a 5% CO_2 atmosphere and 95 % humidity.

All experiments were performed with the approval of the Regional Ethics Committee of Pirkanmaa Hospital District for the use of hiPSCs in these studies (R14023). The HiPSC line was under frequent quality control assessment of gene and protein expression analysis and karyotype and mycoplasma assays.

2.6. Neuronal cell seeding to the scaffolds

At day 32, the maturing neuronal cells were detached with Accutase (Life Technologies, USA) for use in experiments. In all 3D samples, cells were encapsulated into the Col1 hydrogel at a final concentration of 2.5 × 10^6 cells/mL. The layered 3D scaffold samples were cultured in 6-well plates (Nunc, Nunclon, ThermoFisher Scientific). After the last electrospinning round, the samples (layered 3D scaffold on the coverslip) were carefully detached from the glass substrate, glass microscope slide, and moved to the well plate, and NMM was added. CellCrown™6-well inserts (Scaffdex, Tampere, Finland) were used to keep samples on the bottom of the wells. The 2D fiber samples were prepared by removing the coverslips covered with fibers from the microscope slide, transferring them to 6-well plates, coating the fibers with Col1 and plating the cells at a density of 40 000 cells/cm^2 on top of the coated fibers. Additionally, CellCrown™6-well inserts were used. In contrast, the 3D hydrogel samples were casted on glass bottom 24-well plates (MatTek Corporation, Ashland, MA, USA).

All the cell samples were cultured in NMM supplemented with 0.5 % penicillin to prevent contamination. The medium was changed three times a week. Cell experiments were conducted for two weeks. All experiments were repeated twice with at least four parallel samples in each group.

2.7. Immunocytochemistry

For identification of the cells, immunocytochemical staining was performed following previously optimized protocols for 3D samples (Koivisto et al., 2017) and 2D fibers (Lappalainen et al., 2010) with minor modifications. Briefly, 3D cultured cells were fixed with 4 % paraformaldehyde for 60 min, and nonspecific staining was blocked by incubation with 10 % normal donkey serum, 0.1 % Triton-X 100, and 1% bovine serum albumin (BSA, all from Sigma-Aldrich) for 60 min at RT.

Primary antibodies against β-tubulin III (β-tub, mouse, 1:1000, Sigma-Aldrich) and microtubule-associated protein 2 (MAP2, rabbit, 1:400, Millipore) were incubated on cell samples for 3 days on a shaker at 4 °C. The samples were washed with 1% BSA in PBS for two days and washing solution was changed in total five times during this time. Then samples were incubated with secondary antibodies (conjugated with Alexa Fluor 488 or 568, 1:400, Thermo Fisher Scientific) for 24 h on a shaker at 4 °C. The 2D samples were fixed with 4 % paraformaldehyde for 15 min, and nonspecific staining was blocked by incubation with 10 % normal donkey serum, 0.1 % Triton-X 100, and 1% BSA for 45 min at RT. Primary antibodies against β-tub (1:1000) and MAP2 (1:400) were incubated with cell samples for 24 h on a shaker at 4 °C. The samples were washed with 1% BSA in PBS and incubated with secondary antibodies (conjugated with Alexa Fluor 488 or 568, 1:400) for 1 h on a shaker at 4 °C.

All the samples were incubated with PBS including 4′,6-diamidino-2-phenylindole (DAPI, 1:5000, Sigma-Aldrich) for 3 h at RT and then were washed with PBS. The layered 3D scaffold and 2D fiber samples were mounted with Prolong Gold with DAPI and 3D hydrogel samples with Vectashield (Vector Laboratories, England).

2.8. Imaging

Plain fluorescent fibers were imaged with an Olympus IX51 inverted microscope and an Olympus DP30BW digital camera (Olympus Corporation, Japan, Tokyo). All immunocytochemical samples were imaged with a Zeiss LSM 780 confocal microscope (Carl Zeiss AG, Oberkochen, Germany) using a 25× objective (N.A. = 0.80, Zeiss LD LCI Plan-Apochromat, pixel size 0.3 × 0.3 μm, Carl Zeiss). For Z-stacks, slice range was set to 0.5 μm. In each group, four parallel samples and three separate areas/sample were imaged.

2.9. Data analysis

Deconvolution of the confocal microscope images was performed with Hyugens Essential software (Scientific Colume Imaging B.V., Hilversum, Netherlands). To visualize cell growth, colors corresponding to the fluorescent light wavelength were added, and different channels were merged with ImageJ software (U.S. National Institutes of Health, Bethesda, MD, USA). From these images, maximum intensity projections of the desired thickness from 3D stacks were formed. Fine tuning of the images for visualization was performed with Adobe Photoshop (Adobe Systems Inc., San Jose, CA).

For the orientation analysis, all analyzed images were tilted so that fibers were mainly along the x-axis. Moreover, the information from the images was split into two separate image layers: green (MAP2) and red (β-tub) channels, which were combined into one image layer (cell image layer), and the fiber channel (white) was in another layer (fiber image layer, see Supplementary Information 1 and Supplementary Fig. 3). Thereafter, regions of interest (ROIs), defined as single cells, were selected from cell image layers from the experimental groups: layered 3D, 3D hydrogel and 2D fiber. The selection was performed blindly with respect to the experimental group. All separate and clear individual cells were selected as ROIs. From each group, ROIs were selected from at least 7 images, and at least 50 ROIs were included in each group. Coherency and main orientation angle were measured from each ROI using ImageJ plugin OrientationJ (Püspöki and Storath, 2016). Additionally, a color survey map from OrientationJ was used for data visualization.

Data are presented as the mean ± standard deviation (SD), and statistical significance was calculated with the Kruskal-Wallis test with Dunn's multiple comparison *ad hoc*-test. A p-value < 0.05 was considered significant.

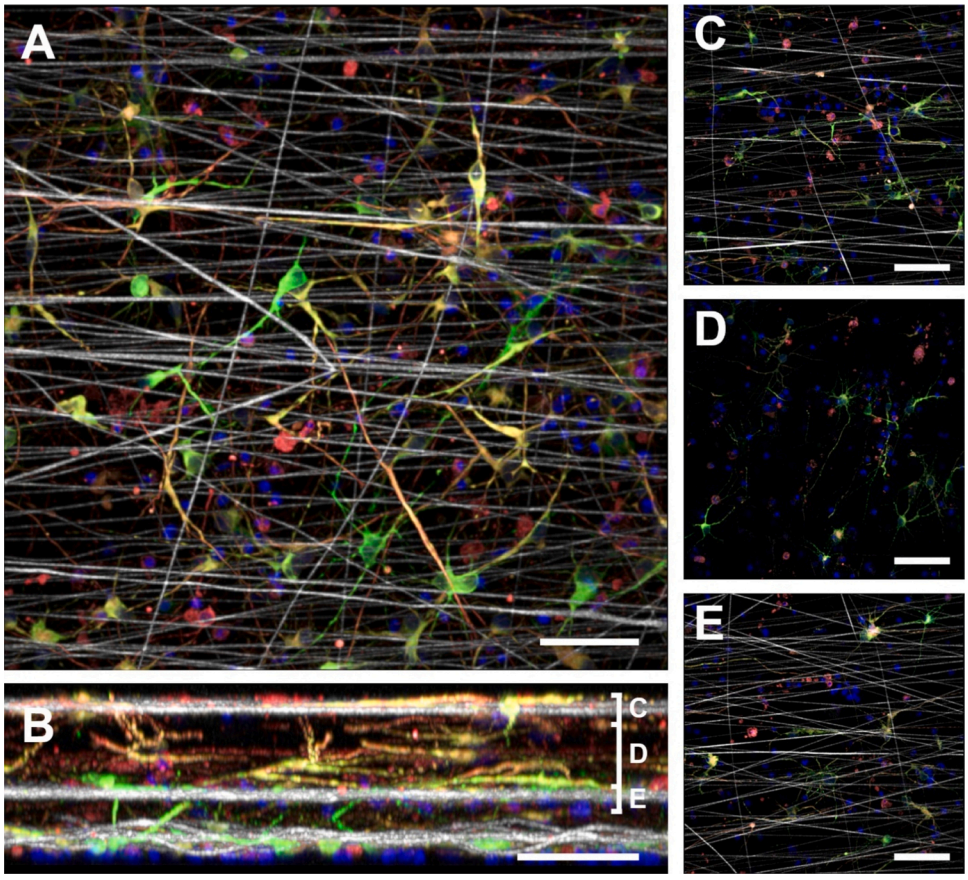

Fig. 3. hPSC-derived neurons cultured in layered 3D fiber-hydrogel scaffolds. A) Top view of the hPSC-derived neurons growing throughout the layered 3D scaffold. The scale bar is 50 μm. B) Cross section of hPSC-derived neurons growing in a layered 3D scaffold showing β-tub- and MAP2-positive neurons in every layer. The scale bar is 50 μm. C)-E) Maximum intensity projections of the z-stack (top view) near separate layers: C) and E) separate fiber layers and D) a hydrogel layer between the fiber layers. Side view of layer C)-E) is marked as a line segment in image B). Scale bars are 100 μm. In the images, red indicates β-tub, green indicates MAP2 and blue indicates DAPI.

3. Results

3.1. Preparation of the layered 3D scaffold

The novelty of the present technique is the assembly of the scaffold so that the structural components, fibers and hydrogel are prepared alternately one after each other in the same process. Hence, the first PLA fiber layer was electrospun on the glass substrate, and the first hydrogel layer was cast on top of it. Then, the next fiber layer was electrospun directly on the freshly prepared hydrogel layer. Altogether, three rounds of electrospinning fibers and two hydrogel gelation periods took approximately two hours. In practice, there were two samples per microscopy slide processed at the same time and several microscopy slides could be processed sequentially. A unique, fork-shaped, rotating collector collected the fibers and transferred them on the glass substrate to form the fiber layer (Fig. 2A). Fluorescent nanoparticles were added to the polymer solution prior to electrospinning, which resulted in capturing the particles inside the PLA fibers. Fluorescent nanoparticles made it easy to visualize the fibers in 3D samples (Fig. 2B). The produced electrospun fibers were characterized with FE-SEM. The average fiber diameter was 600 nm (±152 nm), and the distribution of the diameters is shown as a histogram in Fig. 2C. Fluorescent nanoparticles did not

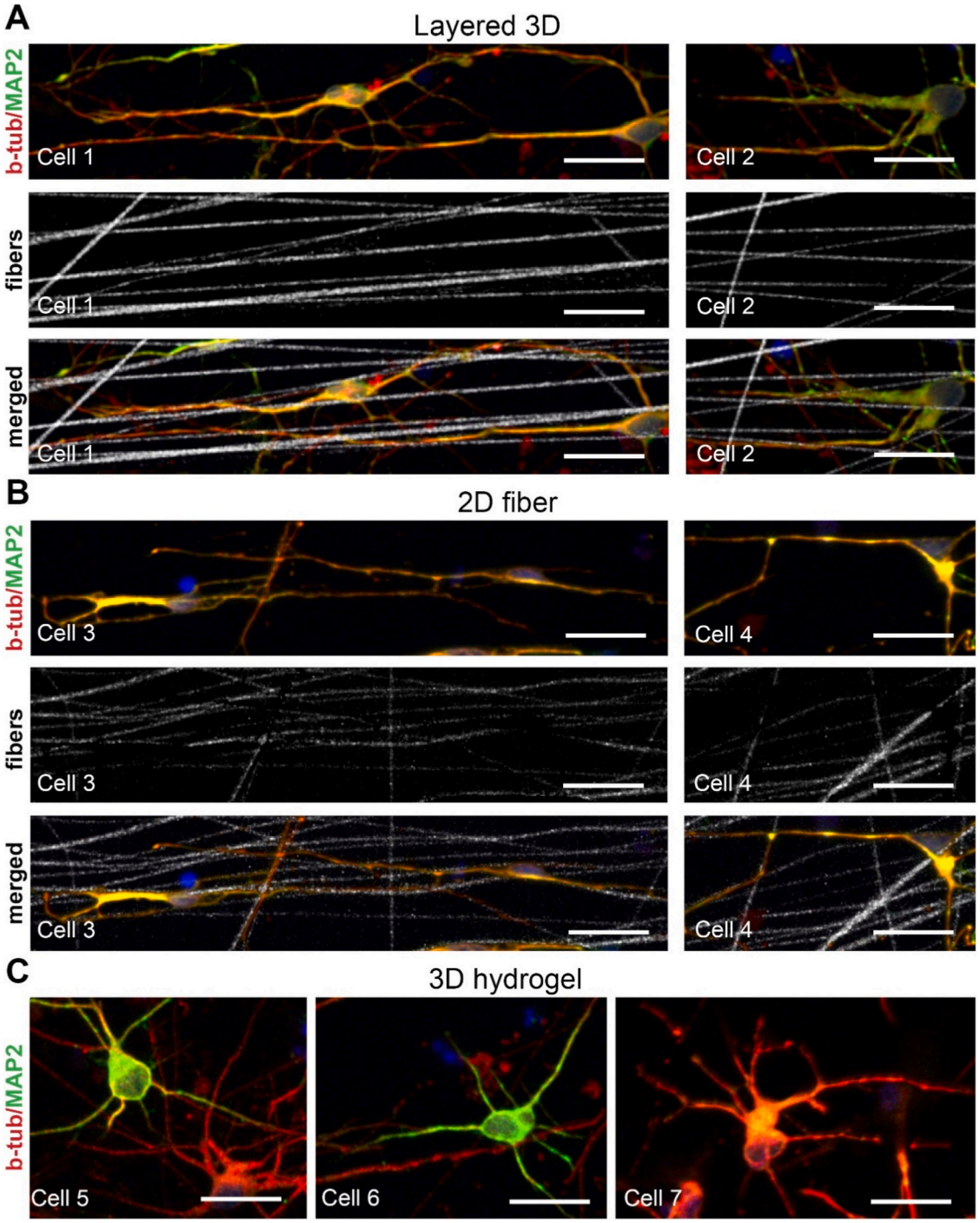

Fig. 4. Neuronal cell orientation. A) Reconstructed z-stacked 3D images of hPSC-derived neurons growing within or near the fiber layer in a layered 3D scaffold. B) hPSC-derived neurons growing on 2D fibers. C) hPSC-derived neurons growing in 3D hydrogel (control sample). Scale bars 25 μm.

affect the surface topography of the fibers, as shown by FE-SEM images (Supplementary Fig. 4). Layer-by-layer construction of the 3D scaffold with PLA fibers and Col1 hydrogel layers was successfully performed. The layered 3D scaffold and its different layers are introduced schematically in Fig. 2D. The scaffold has five layers in total: three separate fibers containing layers (e.g. Fig. 2E and 2 G) and two hydrogel layers (e.g. Fig. 2F).

3.2. Growth of neuronal cells inside the layered 3D scaffold

Layered 3D scaffolds containing human neurons were cultured for two weeks (Fig. 3A). In the layered 3D scaffold, cells spread throughout the sample (Fig. 3B). Typically, the scaffold height varied between 60 and 90 μm. As the process is not completely controllable, some variation was seen both in the whole scaffold and layer thicknesses. A cross-section of the scaffold (Fig. 3C) clearly shows three separate layers containing fibers. Overall, the fibers were embedded in the hydrogel, and accompanying neurons expressed β-tub and MAP2 (see Supplementary video 2). Different layers were observed separately as maximum intensity projections of the confocal microscopy images (Fig. 3D–F). Again, two separate fibers containing layers are presented here as well as the hydrogel layer between them. Cell growth was good in the scaffolds, and cells had typical neuronal morphology and protein expression.

3.3. Cell orientation and analysis

Cell orientation was evaluated in the three experimental groups: layered 3D, 2D fiber and 3D hydrogel samples. Representative images of single cells from each sample group are shown in Fig. 4. In general, neuronal processes, the neurites, seem to elongate further from the soma when they contacted the fiber and started to grow along it.

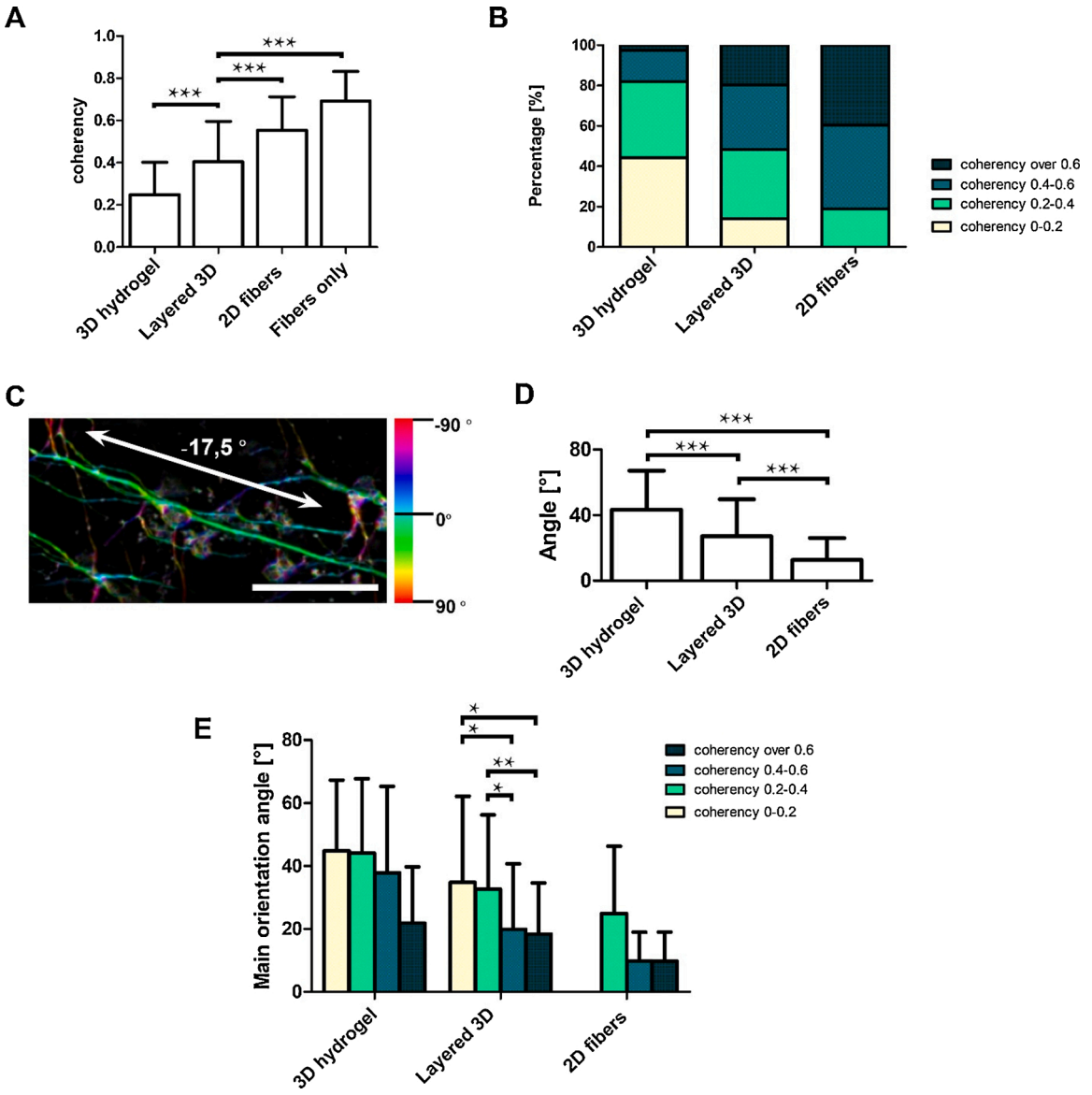

Fig. 5. Cell orientation analysis. A) Coherency measured from ROIs in each group. The coherency value is set from 0.1. to 1.0, where 1.0 is the maximal coherency, n = 53-210 per group. B) Proportion of measured cells (ROIs) in each group divided into segments: very low coherency (0.0-0.2), low coherency (0.2-0.4), high coherency (0.4-0.6) and very high coherency (< 0.6), n = 53-183 per group. C) Representative image of the OrientationJ analysis in which the cell is pseudocolored using orientation information. The main orientation angle of the ROI is marked as a white arrow. D) The main orientation angle of each ROI. Data were plotted as the average absolute value of the main orientation angle, n = 53-183 per group. E) The main orientation angle of each ROI with respect to coherency segments. Data were plotted as the average absolute value of the main orientation angle divided into very low, low, high or very high coherency, similar to B). The scale bar is 50 μm. All the data are represented as the mean ± SD, and $p < 0.05$ was considered significant. * represents $p < 0.05$, and *** represents $p < 0.001$.

Consequently, cell orientation relative to fiber orientation was observed in both samples containing fibers: layered 3D scaffolds (Fig. 4A) and 2D fibers (Fig. 4B). Of these, the cells growing on the 2D fibers followed the fibers more precisely compared to cells grown in layered 3D scaffolds. In contrast, cells in 3D hydrogel samples did not grow in any specific direction (Fig. 4C, see also Supplementary Fig. 5).

For cell coherency and orientation analysis, ROIs were selected around the individual, clear cells (as well as the corresponding area from the fiber image layer, see Supplementary Information 1). The coherency of each ROI was analyzed. In general, the results of the analysis were very logical. The electrospun fiber sample (fibers only) showed the highest coherency (mean 0.692, Fig. 5A), while the ROIs (cells) in 3D hydrogel samples showed the least coherency (mean 0.249). Importantly, cells in the fiber layer in layered 3D samples were significantly more coherent (0.405, $p < 0.001$) than cells in 3D hydrogel samples, and they were significantly less coherent than cells in 2D fiber samples (0.554, $p < 0.001$). Based on the coherency data, analyzed ROIs were divided into four segments within each experimental group (low coherency, 0−0.2; medium coherency, 0.2−0.4; high coherency, 0.4−0.6; and very high coherency, < 0.6). Only experimental groups containing cells were included in the analysis. The results showed that the percentage of ROIs included in the high coherency segment was higher in the 3D layered group (19.7 %) than in the 3D hydrogel group (2.5 %), and it was lower than in the 2D fiber group (39.6 %, Fig. 5B). Following the same trend, the percentage of the ROIs included in the lowest coherency segment was lower in the layered 3D group (14.0 %) than the 3D hydrogel group (44.3 %), and it was higher than that of the 2D fiber group (0 %, Fig. 5B).

Next, the main orientation angles of the ROIs were analyzed. In Fig. 5C, one ROI is shown as a pseudocolored image based on orientation angle elements, and the main orientation angle is marked with a white arrow. In general, the main orientation angle was significantly lower (closer to 0, more aligned along the fibers) in the layered 3D group than in the 3D hydrogel group, but it was higher than in the 2D fiber group (Fig. 5D). This showed a similar trend as the coherency data. Specifically, the main orientation angle was compared according to the coherency segments shown in Fig. 5B (Fig. 5E). Interestingly, the main orientation angle between different coherency segments differed significantly only in layered 3D samples. There, lower coherency segments (0−0.2 and 0.2−0.4) have significantly higher main orientation angles than the high coherency segments (coherency > 0.4), as shown in Fig. 5E.

4. Discussion

In the present study, the objective was to develop a layered 3D scaffold consisting of hPSC-derived neuronal cells to achieve more CNS microenvironment mimicking in vitro model. Furthermore, this scaffold is also applicable for in vivo TE, e.g., for spinal cord injury (Schaub et al., 2016). The construction method combined highly aligned electrospun PLA fibers and cells containing collagen 1 hydrogel in a single process that produced a layer-by-layer 3D scaffold. hPSC-derived neurons were successfully cultured in the scaffold for two weeks. Cell orientation in layered 3D scaffolds was evaluated and compared to 2D fiber scaffolds and 3D hydrogel scaffolds without fibers. The neurons growing near fiber layers showed increased directional orientation. Thus, we demonstrated a versatile method for the preparation of layered 3D scaffolds for neuronal cells. Moreover, cell orientation along the embedded fibers indicated a successful preparation of a 3D scaffold that offers guiding cues for neuronal cells.

The tissue in vivo contains guidance cues such as elongated radial glial cells, which control cell growth and alignment (Hopkins et al., 2015; Kaur et al., 2020). To mimic these fibrous cues, electrospun fibers are widely used, as their size range can be adjusted to correspond to a range that cells respond to (Haider et al., 2018; Schaub et al., 2016). Our electrospinning technique resulted in highly aligned fibers with an average diameter of 600 nm. This is in the range of PLA fiber diameters shown to promote neuronal viability, directionality and neurite outgrowth (He et al., 2010; Yang et al., 2005). Conventional electrospinning results in a random, nonwoven fiber mat. Parallel aligned fibers, on the other hand, are obtained with special types of collectors in which the alignment is controlled by using mechanical, electrical or magnetic forces (Xue et al., 2019). Here, the unique, fork-shaped, rotating dual-electrode collector exploits two of these forces: electrical manipulation between two parallel electrodes separated by an air gap and mechanical pulling of the fibers by rotation (Grigoryev and Levon, 2018). The polymer jet ejected from the needle is attracted to that electrode, which has the shortest distance to the needle at each time point. When rotating, the collector mechanically transfers the fibers one at the time to the substrate, which in this case is the glass substrate that is horizontally located in the void between the electrodes. With this approach, it is possible to cast a collagen solution on the substrate, and after a short gelation time, the fibers can be spun on top of or partially inside the forming hydrogel. Importantly, this collector made it possible to include hPSC-derived neurons into hydrogel during the electrospinning process without damage to the cells. Previous multilayered composite structures used mainly electrospun fiber mats attached to the different frames or rings embedded into the hydrogel in a separate process (McMurtrey, 2014; Weightman et al., 2014b; Yang et al., 2011). This limits the fibers strictly to one plain in the z-direction, which is relative to mimicking tissues with layered structures, e.g., the skin or cornea (Coburn et al., 2011). The technique used here forms all the layers in one process; thus, fibers are not limited strictly to the single plane, permitting them to distribute into the hydrogel to some extent, mimicking the fibrous nature of guidance cues in tissue. With the method presented here, it is possible to vary the characteristics (e.g., fiber diameter, fiber density, layer thickness and hydrogel layer thickness) of the 3D layered scaffold according to specific needs. In other point of few it would be possible to incorporate different cell types, use different hydrogel stiffnesses of even different hydrogels in the different hydrogel layers. Thus, the scaffold could be used to model real defects in CNS, for example spinal cord injury or traumatic brain injury in the cortex (Kumaria, 2017; Weightman et al., 2014b). Taken together, the composite scaffolds produced with this method can be used as microenvironment-mimicking scaffolds that fulfil both requirements: fibrous nature and gelatinous hydrogel matrix.

In layer-by-layer structures, visible light scatters from the translucent fibers, distorting the deconstruction of the 3D image. To overcome this issue, we added fluorescent nanoparticles to the PLA solution to enable visualization of the fibers, which were imaged with a 660 nm wavelength. To date, 3D images of fiber-hydrogel composite structures have only seldom been presented in the literature, even though fluorescent fibers have been prepared to some extent (Weightman et al., 2014a, b). With our approach, we were able to visualize the layered 3D scaffold for subsequent orientation analysis.

When producing tissue mimicking in vitro models, a suitable cell source, a CNS mimicking scaffold and a sufficient long culture time for neuronal cell maturation and network formation are needed (Lam et al., 2020; Tang-Schomer et al., 2014). In previous studies, the cell culture times varied from a few days (McMurtrey, 2014) to even months (Tang-Schomer et al., 2014). In addition, earlier studies have mostly utilized animal-derived neuronal cells (Lee et al., 2016; Soliman et al., 2018; Weightman et al., 2014a) or human-derived cancer cells (McMurtrey, 2014), whereas the use of hPSC-derived cells has not been reported. Here, we used hPSC-derived neuronal cells, a cell supportive hydrogel-fiber scaffold and a two-week culture time. Despite rather demanding sample preparation conditions during the electrospinning rounds, neurons survived and grew in every layer of the scaffold. In previous studies, electrospun fibers have been modified with various polymer or protein functionalizations to create additional cell adhesion sites (Lee et al., 2016; McMurtrey, 2014; Puschmann et al., 2014; Wieringa et al., 2019). Here, the cells oriented along the fibers without

any additional functionalization. This finding is consistent with our previous data, which showed that untreated PLA fiber mesh supports human neurite outgrowth in a manner equivalent to that of laminin-coated surfaces (Ylä-Outinen et al., 2010). In the future, this kind of scaffold can be used with several CNS cell types (e.g., neurons and astrocytes), and fibers can act as guidance cues or limiting factors for particular cell types.

Electrospun fibers have been shown to offer contact guidance for neuronal cells as well as to affect their morphology and neurite outgrowth, as they resemble naturally occurring aligned neurite bundles (D'Amato et al., 2019; Kijeńska et al., 2012; Roach et al., 2010). Previously, the cellular response to fibers was analyzed by neurite directionality and alignment of neurites. In practice, it has been realized by determining the cell orientation along the fibers, cell morphologies and neurite lengths (Hyysalo et al., 2017; McMurtrey, 2014; Weightman et al., 2014a). In this study, the OrientationJ plugin of ImageJ software was used to analyze the cell orientation in detail (Püspöki and Storath, 2016). ROIs identified with reliable neuronal markers were used to analyze coherency and main orientation angle. Based on the analysis, the neurons interacted with the fibers by adopting elongated morphology and directed neurite growth in close proximity with the fibers. It also seems that size of the somas is affected with the layered 3D hydrogel environment compared to 3D hydrogel environment. The cell orientation analysis was based on coherency and orientation angle measurements. When comparing the experimental groups, the coherency was significantly higher in 2D fibers than in 3D fibers. For more detailed analysis, we wanted to compare the alignment of cell orientation to fiber alignment. The average main orientation angle analysis showed a similar trend as the coherency analysis, meaning that cells grown on 2D fiber had a lower main orientation angle (closer to fiber orientation) than the cells grown in layered 3D scaffolds. Hence, neither the coherency nor orientation angle of the cells in the layered 3D scaffold was as good as the corresponding values of the cells grown on the 2D fibers. Previously, it has been shown that for cells to sense the presence of an untreated fiber layer in 3D, hPSC-derived neurons need initially to be brought into close contact (< 10 μm) with the fibers (Hyysalo et al., 2017). Therefore, neuronal cell orientation followed the direction of the fibers more easily when growing on the 2D-treated fiber surface compared to the 3D environment (Hyysalo et al., 2017). However, better neurite tracking and subsequent neuron orientation were reported in 3D scaffolds compared to 2D scaffolds when using sparse and treated fiber layers (McMurtrey, 2014). Here, cells cultured on 2D fibers were in very close contact with fibers, whereas cells in layered 3D scaffolds had more degrees of freedom for growth directions. Previously, to overcome this issue, cells were seeded directly on each fiber layer before casting the hydrogel (A. Weightman et al., 2014a). Thus, this showed that cells cultured in layered 3D scaffolds followed the fibers to some extent, but not as closely as cells cultured on the 2D fibers. Additionally, the applied method offered a robust and fast way to analyze cell directionality and orientation in 3D.

Previously, it was shown that with a sparse fiber layer, even a single fiber could create enough guiding cues for direct neurite tracking in 3D (McMurtrey, 2014). In this study, the produced fiber layers in layered 3D scaffolds were left intentionally sparse, as it is important to ensure the infiltration of the cells throughout the structure. Fiber layers or fiber bundles that are too dense may lead to situations where cells settle on the fibers and grow along them without having direct interaction with them (McMurtrey, 2014). Here, in a layered 3D scaffold, the cells in close proximity with the fibers sense the guidance cues, so they develop an elongated shape. In contrast, cells in the hydrogel layer between the fiber layers remained more stellate shaped, and orientation into any particular direction was not observed. Additionally, coherency and orientation angle analysis of layered 3D and 3D hydrogel groups supported these findings as previous studies with layer-by-layer scaffolds (McMurtrey, 2014; A. Weightman et al., 2014a). On the other hand, the surrounding hydrogel, especially its number of cell responsive binding sites, can have a major effect on the cell orientation along the fibers inside the 3D scaffold (McMurtrey, 2014). Here, we used collagen 1, which by itself can support cells (Allodi et al., 2011; Ylä-Outinen et al., 2019), but it does not disturb the guidance effect of fibers in the layered 3D scaffold. Apart from self-assembling collagen, other 3D hydrogel matrices could also be used. For example, in the structures constructed by layer-by-layer method alginate with ionic crosslinking (Wu et al., 2015) has already been used. Also, hydrogels with chemical crosslinking would be possible to use as long as gelation time is sufficient for even spreading on the fibers. However, photocurable hydrogels crosslinked with UV or visible light would be difficult to integrate to the system. However, cells in the layered 3D scaffold were considerably more oriented than those in the 3D hydrogel alone. Additionally, despite the debate about the hydrophobicity of PLA fibers (Schaub et al., 2016), neurons in layered 3D scaffolds grew, followed and interacted with the fibers. To conclude, the results showed that fibers had a greater effect on the cells growing on the layered 3D scaffold than the cells growing in the 3D hydrogel.

Here, we introduced a method to produce a layered scaffold for neuronal cells to mimic CNS microenvironment by alternating a soft hydrogel matrix and fibrous guidance cues. The produced scaffold was demonstrated as a successful 3D platform for the long-term culture of hPSC-derived neuronal cells. Importantly, embedded fibers in the scaffold enhanced cell elongation and directed neurite growth. This layered 3D scaffold is a useful model for in vitro and in vivo neuronal TE applications.

Funding

This work was supported by Academy of Finland, Finland (nos. 286990, 326436 for LYO, 312414, 311017 for SN) and The Instrumentarium Science Foundation, Finland (200011 for LH).

Declaration of Competing Interest

The authors declare no conflict of interest.

CRediT authorship contribution statement

Laura Honkamäki: Conceptualization, Investigation, Visualization, Methodology, Data curation, Writing - original draft, Funding acquisition. **Tiina Joki:** Investigation, Methodology, Writing - review & editing. **Nikita A. Grigoryev:** Resources, Methodology, Writing - review & editing. **Kalle Levon:** Conceptualization, Resources, Methodology, Writing - review & editing. **Laura Ylä-Outinen:** Conceptualization, Methodology, Visualization, Formal analysis, Writing - original draft, Supervision, Funding acquisition. **Susanna Narkilahti:** Resources, Supervision, Project administration, Writing - review & editing, Funding acquisition.

Acknowledgements

The authors acknowledge the Biocenter Finland (BF) and Tampere Imaging Facility (TIF), Tampere Microscopy Center and Tampere Facility of iPS Cells for their services.

Appendix A. Supplementary data

Supplementary material related to this article can be found, in the online version, at doi:https://doi.org/10.1016/j.jneumeth.2020.109043.

References

Allodi, I., Guzmán-Lenis, M.S., Hernàndez, J., Navarro, X., Udina, E., 2011. In vitro comparison of motor and sensory neuron outgrowth in a 3D collagen matrix. J. Neurosci. Methods 198, 53–61. https://doi.org/10.1016/j.jneumeth.2011.03.006.

Bandtlow, C.E., Zimmermann, D.R., 2000. Proteoglycans in the developing brain: new conceptual insights for old proteins. Physiol. Rev. https://doi.org/10.1152/physrev.2000.80.4.1267.

Benam, K.H., Dauth, S., Hassell, B., Herland, A., Jain, A., Jang, K.-J., Karalis, K., Kim, H. J., MacQueen, L., Mahmoodian, R., Musah, S., Torisawa, Y., van der Meer, A.D., Villenave, R., Yadid, M., Parker, K.K., Ingber, D.E., 2015. Engineered in vitro disease models. Annu. Rev. Pathol. Mech. Dis. 10, 195–262. https://doi.org/10.1146/annurev-pathol-012414-040418.

Berzat, A., Hall, A., 2010. Cellular responses to extracellular guidance cues. EMBO J. https://doi.org/10.1038/emboj.2010.170.

Bosworth, L.A., Turner, L.-A., Cartmell, S.H., 2013. State of the art composites comprising electrospun fibres coupled with hydrogels: a review. Nanomed. Nanotechnol. Biol. Med. 9, 322–335. https://doi.org/10.1016/J.NANO.2012.10.008.

Cao, H., Liu, T., Chew, S.Y., 2009. The application of nanofibrous scaffolds in neural tissue engineering. Adv. Drug Deliv. Rev. 61, 1055–1064. https://doi.org/10.1016/j.addr.2009.07.009.

Cembran, A., Bruggeman, K.F., Williams, R.J., Parish, C.L., Nisbet, D.R., 2020. Biomimetic materials and their utility in modeling the 3-dimensional neural environment. ISCIENCE 23, 100788. https://doi.org/10.1016/j.isci.

Chen, Z., 2019. Common cues wire the spinal cord: axon guidance molecules in spinal neuron migration. Semin. Cell Dev. Biol. https://doi.org/10.1016/j.semcdb.2017.12.012.

Choi, J.H., Cho, H.Y., Choi, J.W., 2017. Microdevice platform for in vitro nervous system and its disease model. Bioengineering 4. https://doi.org/10.3390/bioengineering4030077.

Coburn, J., Gibson, M., Bandalini, P.A., Laird, C., Mao, H.-Q., Moroni, L., Seliktar, D., Elisseeff, J., 2011. Biomimetics of the extracellular matrix: an integrated three-dimensional fiber-hydrogel composite for cartilage tissue engineering. Smart Struct. Syst. 7, 213–222. https://doi.org/10.12989/sss.2011.7.3.213.

D'Amato, A.R., Puhl, D.L., Ziemba, A.M., Johnson, C.D.L., Doedee, J., Bao, J., Gilbert, R. J., 2019. Exploring the effects of electrospun fiber surface nanotopography on neurite outgrowth and branching in neuron cultures. PLoS One 14, 1–18. https://doi.org/10.1371/journal.pone.0211731.

Grigoryev, N.A., Levon, K., 2018. Novel method of electrospinning; rotating dual electrode collector design. J. Microelectromech. Syst. 27, 312–320. https://doi.org/10.1109/JMEMS.2018.2796300.

Haider, A., Haider, S., Kang, I.K., 2018. A comprehensive review summarizing the effect of electrospinning parameters and potential applications of nanofibers in biomedical and biotechnology. Arab. J. Chem. https://doi.org/10.1016/j.arabjc.2015.11.015.

He, L., Liao, S., Quan, D., Ma, K., Chan, C., Ramakrishna, S., Lu, J., 2010. Synergistic effects of electrospun PLLA fiber dimension and pattern on neonatal mouse cerebellum C17.2 stem cells. Acta Biomater. 6, 2960–2969. https://doi.org/10.1016/j.actbio.2010.02.039.

Hopkins, A.M., DeSimone, E., Chwalek, K., Kaplan, D.L., 2015. 3D in vitro modeling of the central nervous system. Prog. Neurobiol. 125, 1–25. https://doi.org/10.1016/J.PNEUROBIO.2014.11.003.

Huang, G., Li, F., Zhao, X., Ma, Y., Li, Y., Lin, M., Jin, G., Lu, T.J., Genin, G.M., Xu, F., 2017. Functional and biomimetic materials for engineering of the three-dimensional cell microenvironment. Chem. Rev. https://doi.org/10.1021/acs.chemrev.7b00094.

Hyvärinen, T., Hyysalo, A., Kapucu, F.E., Aarnos, L., Vinogradov, A., Eglen, S.J., Ylä-Outinen, L., Narkilahti, S., 2019. Functional characterization of human pluripotent stem cell-derived cortical networks differentiated on laminin-521 substrate: comparison to rat cortical cultures. Sci. Rep. 9, 17125. https://doi.org/10.1038/s41598-019-53647-8.

Hyysalo, A., Ristola, M., Joki, T., Honkanen, M., Vippola, M., Narkilahti, S., 2017. Aligned Poly(ε-caprolactone) nanofibers guide the orientation and migration of human pluripotent stem cell-derived neurons, astrocytes, and oligodendrocyte precursor cells in vitro. Macromol. Biosci. 17, 1600517. https://doi.org/10.1002/mabi.201600517.

Johnson, C.D., D'Amato, A.R., Puhl, D.L., Wich, D.M., Vesperman, A., Gilbert, R.J., 2018. Electrospun fiber surface nanotopography influences astrocyte-mediated neurite outgrowth. Biomed. Mater. 13, 054101. https://doi.org/10.1088/1748-605X/aac4de.

Jun, I., Han, H.S., Edwards, J.R., Jeon, H., 2018. Electrospun fibrous scaffolds for tissue engineering: Viewpoints on architecture and fabrication. Int. J. Mol. Sci. 19 https://doi.org/10.3390/ijms19030745.

KarbalaeiMahdi, A., Shahrousvand, M., Javadi, H.R., Ghollasi, M., Norouz, F., Kamali, M., Salimi, A., 2017. Neural differentiation of human induced pluripotent stem cells on polycaprolactone/gelatin bi-electrospun nanofibers. Mater. Sci. Eng. C 78, 1195–1202. https://doi.org/10.1016/j.msec.2017.04.083.

Karvinen, J., Joki, T., Ylä-Outinen, L., Koivisto, J.T., Narkilahti, S., Kellomäki, M., 2018. Soft hydrazone crosslinked hyaluronan- and alginate-based hydrogels as 3D supportive matrices for human pluripotent stem cell-derived neuronal cells. React. Funct. Polym. 124, 29–39. https://doi.org/10.1016/J.REACTFUNCTPOLYM.2017.12.019.

Kaur, N., Han, W., Li, Zhuo, Madrigal, M.P., Shim, S., Pochareddy, S., Gulden, F.O., Li, M., Xu, X., Xing, X., Takeo, Y., Li, Zhen, Lu, K., Imamura Kawasawa, Y., Ballester-Lurbe, B., Moreno-Bravo, J.A., Chédotal, A., Terrado, J., Pérez-Roger, I., Koleske, A. J., Sestan, N., 2020. Neural stem cells direct axon guidance via their radial fiber scaffold. Neuron 107, 1197–1211. https://doi.org/10.1016/j.neuron.2020.06.035 e9.

Kiamehr, M., Klettner, A., Richert, E., Koskela, A., Koistinen, A., Skottman, H., Kaarniranta, K., Aalto-Setälä, K., Juuti-Uusitalo, K., 2019. Compromised barrier function in human induced pluripotent stem-cell-derived retinal pigment epithelial cells from type 2 diabetic patients. Int. J. Mol. Sci. 20, 3773. https://doi.org/10.3390/ijms20153773.

Kijeńska, E., Prabhakaran, M.P., Swieszkowski, W., Kurzydlowski, K.J., Ramakrishna, S., 2012. Electrospun bio-composite P(LLA-CL)/collagen I/collagen III scaffolds for nerve tissue engineering. J. Biomed. Mater. Res. - Part B Appl. Biomater. 100 B, 1093–1102. https://doi.org/10.1002/jbm.b.32676.

Koivisto, J.T., Joki, T., Parraga, J.E., Pääkkönen, R., Ylä-Outinen, L., Salonen, L., Jönkkäri, I., Peltola, M., Ihalainen, T.O., Narkilahti, S., Kellomäki, M., 2017. Bioamine-crosslinked gellan gum hydrogel for neural tissue engineering. Biomed. Mater. 12, 025014. https://doi.org/10.1088/1748-605X/aa62b0.

Kumaria, A., 2017. In vitro models as a platform to investigate traumatic brain injury. ATLA Altern. to Lab. Anim. 45, 201–211. https://doi.org/10.1177/026119291704500405.

Lam, D., Enright, H.A., Peters, S.K.G., Moya, M.L., Soscia, D.A., Cadena, J., Alvarado, J. A., Kulp, K.S., Wheeler, E.K., Fischer, N.O., 2020. Optimizing cell encapsulation condition in ECM-Collagen I hydrogels to support 3D neuronal cultures. J. Neurosci. Methods 329, 108460. https://doi.org/10.1016/j.jneumeth.2019.108460.

Lappalainen, R.S., Salomäki, M., Ylä-Outinen, L., Heikkilä, T.J., Hyttinen, J.A., Pihlajamäki, H., Suuronen, R., Skottman, H., Narkilahti, S., 2010. Similarly derived and cultured hESC lines show variation in their developmental potential towards neuronal cells in long-term culture. Regen. Med. 5, 749–762. https://doi.org/10.2217/rme.10.58.

Lee, S.-J., Nowicki, M., Harris, B., Zhang, L.G., 2016. Fabrication of a highly aligned neural scaffold via a table top stereolithography 3D printing and electrospinning. Tissue Eng. Part A 23, 491–502. https://doi.org/10.1089/ten.tea.2016.0353.

McMurtrey, R.J., 2014. Patterned and functionalized nanofiber scaffolds in three-dimensional hydrogel constructs enhance neurite outgrowth and directional control. J. Neural Eng. 11, 066009. https://doi.org/10.1088/1741-2560/11/6/066009.

Papadimitriou, L., Manganas, P., Ranella, A., Stratakis, E., 2020. Biofabrication for neural tissue engineering applications. Mater. Today Bio. https://doi.org/10.1016/j.mtbio.2020.100043.

Park, S., Park, K., Yoon, H., Son, J., Min, T., Kim, G., 2007. Apparatus for preparing electrospun nanofibers: designing an electrospinning process for nanofiber fabrication. Polym. Int. 56, 1361–1366. https://doi.org/10.1002/pi.2345.

Puschmann, T.B., de Pablo, Y., Zandén, C., Liu, J., Pekny, M., 2014. A novel method for three-dimensional culture of central nervous system neurons. Tissue Eng. Part C Methods 20, 485–492. https://doi.org/10.1089/ten.tec.2013.0445.

Püspöki, Zsuzsanna, Storath, M., S.D, U.M, 2016. Transforms and operators for directional bioimage analysis: a survey. In: De Vos Winnok, H., Munck, S., T.J.-P (Eds.), Focus on Bio-Image Informatics. Springer International Publishing, Cham, pp. 69–93. https://doi.org/10.1007/978-3-319-28549-8_3.

Qiu, B., Bessler, N., Figler, K., Buchholz, M., Rios, A.C., Malda, J., Levato, R., Caiazzo, M., 2020. Bioprinting neural systems to model central nervous system diseases. Adv. Funct. Mater. 1910250. https://doi.org/10.1002/adfm.201910250.

Richardson, J.A., Rementer, C.W., Bruder, J.M., Hoffman-Kim, D., 2011. Guidance of dorsal root ganglion neurites and Schwann cells by isolated Schwann cell topography on poly(dimethyl siloxane) conduits and films. J. Neural Eng. https://doi.org/10.1088/1741-2560/8/4/046015.

Roach, P., Parker, T., Gadegaard, N., Alexander, M.R., 2010. Surface strategies for control of neuronal cell adhesion: a review. Surf. Sci. Rep. https://doi.org/10.1016/j.surfrep.2010.07.001.

Schaub, N.J., Johnson, C.D., Cooper, B., Gilbert, R.J., 2016. Electrospun Fibers for Spinal Cord Injury Research and Regeneration. J. Neurotrauma 33, 1405. https://doi.org/10.1089/NEU.2015.4165.

Soliman, E., Bianchi, F., Sleigh, J.N., George, J.H., Cader, M.Z., Cui, Z., Ye, H., 2018. Aligned electrospun fibers for neural patterning. Biotechnol. Lett. 40, 601–607. https://doi.org/10.1007/s10529-017-2494-z.

Tang-Schomer, M.D., White, J.D., Tien, L.W., Schmitt, L.I., Valentin, T.M., Graziano, D. J., Hopkins, A.M., Omenetto, F.G., Haydon, P.G., Kaplan, D.L., 2014. Bioengineered functional brain-like cortical tissue. Proc. Natl. Acad. Sci. U. S. A. 111, 13811–13816. https://doi.org/10.1073/pnas.1324214111.

Wang, H.B., Mullins, M.E., Cregg, J.M., McCarthy, C.W., Gilbert, R.J., 2010. Varying the diameter of aligned electrospun fibers alters neurite outgrowth and Schwann cell migration. Acta Biomater. 6, 2970–2978. https://doi.org/10.1016/j.actbio.2010.02.020.

Wedeen, V.J., Rosene, D.L., Wang, R., Dai, G., Mortazavi, F., Hagmann, P., Kaas, J.H., Tseng, W.Y.I., 2012. The geometric structure of the brain fiber pathways. Science 80 (335), 1628–1634. https://doi.org/10.1126/science.1215280.

Weightman, A., Jenkins, S., Pickard, M., Chari, D., Yang, Y., 2014a. Alignment of multiple glial cell populations in 3D nanofiber scaffolds: toward the development of multicellular implantable scaffolds for repair of neural injury. Nanomed. Nanotechnol. Biol. Med. 10, 291–295. https://doi.org/10.1016/j.nano.2013.09.001.

Weightman, A.P., Pickard, M.R., Yang, Y., Chari, D.M., 2014b. An in vitro spinal cord injury model to screen neuroregenerative materials. Biomaterials 35, 3756–3765. https://doi.org/10.1016/j.biomaterials.2014.01.022.

Wieringa, B.P., Girao, A., Truckenmuller, R., Welle, A., 2019. A one-step biofunctionalization strategy of electrospun scaffolds enables spatially selective presentation of biological cues. bioRxiv 850875. https://doi.org/10.1101/850875.

Wu, R., Niamat, R., Sansbury, B., Borjigin, M., 2015. Fabrication and evaluation of multilayer nanofiber-hydrogel meshes with a controlled release property. Fibers 3, 296–308. https://doi.org/10.3390/fib3030296.

Xue, J., Wu, T., Dai, Y., Xia, Y., 2019. Electrospinning and electrospun nanofibers: Methods, materials, and applications. Chem. Rev. https://doi.org/10.1021/acs.chemrev.8b00593.

Yang, F., Murugan, R., Wang, S., Ramakrishna, S., 2005. Electrospinning of nano/micro scale poly(l-lactic acid) aligned fibers and their potential in neural tissue engineering. Biomaterials 26, 2603–2610. https://doi.org/10.1016/j.biomaterials.2004.06.051.

Yang, Y., Wimpenny, I., Ahearne, M., 2011. Portable nanofiber meshes dictate cell orientation throughout three-dimensional hydrogels. Nanomed. Nanotechnol. Biol. Med. 7, 131–136. https://doi.org/10.1016/j.nano.2010.12.011.

Ylä-Outinen, L., Harju, V., Joki, T., Koivisto, J.T., Karvinen, J., Kellomäki, M., Narkilahti, S., 2019. Screening of Hydrogels for Human Pluripotent Stem Cell–Derived Neural Cells: Hyaluronan-Polyvinyl Alcohol-Collagen-Based Interpenetrating Polymer Network Provides an Improved Hydrogel Scaffold. Macromol. Biosci. 19 https://doi.org/10.1002/mabi.201900096.

Ylä-Outinen, L., Mariani, C., Skottman, H., Suuronen, R., Harlin, A., Narkilahti, S., 2010. Electrospun Poly(L,D-lactide) Scaffolds Support the Growth of Human Embryonic Stem Cell-derived Neuronal Cells. Open Tissue Eng. Regen. Med. J. https://doi.org/10.2174/1875043501003010001.